

# Modeling and compensation of nonlinear distortion in direct-detection optical Fast-OFDM systems

Luis Carlos Vieira<sup>\*†</sup>, Waseem Ozan<sup>†</sup>, John Mitchell<sup>†</sup>, Izzat Darwazeh<sup>†</sup>

<sup>†</sup>Department of Electronic and Electrical Engineering, University College London (UCL), London, U.K.

<sup>†</sup>Graduate Program in Electrical and Computer Engineering (CPGEI), Federal University of Technology - Paraná (UTFPR), Curitiba, Brazil.  
E-mail: vieira@utfpr.edu.br

**Abstract**—Fast-OFDM based intensity-modulation and direct-detection (IM/DD) has been proposed for the deployment of cost-efficient optical access networks, due to simple implementation and high spectral efficiency. In this work, the generalized memory polynomial (GMP) is firstly applied to model the nonlinear characteristic of IM/DD Fast-OFDM links, including memory effects. After model validation using measured data of a 10-km single mode fiber link, the GMP is used for performance investigations of a combined clipping and digital post-distortion approach to optical Fast-OFDM, considering both 4PAM and 8PAM modulation formats and different number of Fast-OFDM subcarriers. This work firstly reports performance results of optical 8PAM-Fast-OFDM systems using 2PAM-based training signals for digital post-distortion and FFT-based channel estimation. Excellent performance improvements are achieved using the proposed distortion compensation scheme, relative to conventional system implementation.

**Index Terms**—Fast-OFDM, nonlinear modeling, distortion compensation.

## I. INTRODUCTION

Orthogonal frequency division multiplexing (OFDM) based intensity-modulation and direct-detection (IM/DD) is considered a promising solution for high data rate short-reach fiber-optic networks, such as access networks and data centre interconnects. IM/DD OFDM has the advantages of reduced complexity and cost-efficient deployment relative to coherent-detection optical OFDM systems [1], [2]. Nevertheless, in order to enable using quadrature amplitude modulation (QAM)-OFDM with IM/DD, Hermitian transpose is needed at the transmitter side to obtain a real signal at the output of inverse fast Fourier transform (IFFT) [1].

Fast-OFDM [3] is another multicarrier signal and system that has been proposed for IM/DD optical systems [4]–[7], which advantageously offers either 50% bandwidth saving or double the number of data subcarriers within the same bandwidth compared to using conventional OFDM systems. This is achieved by either compressing the frequency spacing between the subcarriers down to  $1/2T$ , where  $T$  is the symbol duration, or sampling faster in comparison to conventional OFDM. Unlike OFDM, Fast-OFDM is a real cosine modulated signal, where inverse discrete cosine transform (IDCT) may be used for generating the real Fast-OFDM signal, and hence there is no need for Hermitian transpose at the transmitter. Thus, IM/DD Fast-OFDM can be considered a suitable solution for high-speed cost-sensitive applications.

In IM/DD links, Fast-OFDM signals may be impaired by

the nonlinearity coming from the electro-optic converters and, in the case of long span links, also by the fiber chromatic dispersion. In the case of Mach–Zehnder modulator (MZM)-based IM/DD DC offset Fast-OFDM, the degree of nonlinear distortion depends on both the bias level and the power level of the input signal, and the MZM is commonly biased at the quadrature point for best linearity [5]. However, even at the quadrature point, the high peaks of a Fast-OFDM signal may reach the nonlinear region of the MZM characteristic. Thus, some peak-to-average power ratio (PAPR) reduction and/or linearization technique might be needed to diminish the level of signal’s distortion.

Clipping the large peaks of a OFDM-based signal is the simplest approach to PAPR reduction, but it may cause additional in-band and out-of-band distortion [8]. Filtering after clipping can be used to reduce the out-of-band distortion. However, the nonlinear distortion that falls within the signal bandwidth can not be filtered out [9]. Adaptive digital predistortion and post-distortion techniques have been proposed for the compensation of nonlinear distortion in optical communication systems [4], [10]–[12]. Digital predistortion is more complex to implement than post-distortion due to the need of an additional feedback link for model identification. In addition, the nonlinearity of the feedback link itself will reduce the predistortion performance [11]. Thus, if the application scenario allows to apply the distortion compensation at the receiver side, post-distortion represents a simpler solution.

In [13], a generalized memory polynomial (GMP) was proposed for digital predistortion of RF power amplifiers. The GMP combines the basic memory polynomial (MP) structure [14] with cross terms between the signal and lagging and/or leading exponentiated envelope terms. In this way, the GMP model is more capable of modeling/compensating the system dynamic nonlinearity in comparison to the MP model.

In this paper, we model the linear and nonlinear characteristics of short-range direct-detection optical Fast-OFDM links based on the GMP model [13] and using a behavioral modeling approach. This is a system approach in which the composite effect of the nonlinearity is modeled by investigating the input-output characteristic of the nonlinear system, based on the baseband versions of the input-output signals. We compare the modeling accuracy of the GMP against that of the well known MP model. We then apply the GMP-based Fast-OFDM model to investigate the performance of an amplitude clipping and polynomial post-distortion scheme for optical Fast-OFDM

links. In our previous work [4], no clipping was employed at the transmitter side and a different channel estimation method was used. In addition, no modeling investigation involving either the MP or GMP model was considered. In contrast to [15], where a time-domain equalization and DCT-based demodulation approach was used for optical Fast-OFDM, FFT-based demodulation and equalization are employed in the current work.

The novelty of the current paper is summarized as follows: (1) the GMP model is applied, for the first time, as a nonlinear model with memory to represent direct-detection optical Fast-OFDM systems; (2) the combined amplitude clipping and digital post-distortion scheme is firstly proposed for optical Fast-OFDM systems; (3) 2PAM-based training signals are firstly applied for digital post-distortion and FFT-based channel estimation of optical 8PAM-Fast-OFDM systems.

## II. SIGNAL MODEL AND SYSTEM DESCRIPTION

### A. Fast-OFDM signal

For a Fast-OFDM system with  $N$  subcarriers, the expression of generating the discrete time signal  $x(n)$  based on IDCT is given by

$$x(n) = \sqrt{\frac{2}{N}} \sum_{k=0}^{N-1} \epsilon(k) s(k) \cos \left[ \frac{\pi(2n+1)k}{2N} \right] \quad (1)$$

where  $n = \{0, 1, 2, \dots, N-1\}$  is the index of time samples in a Fast-OFDM symbol, and  $s(k)$  is the real-valued input data modulated on the  $k^{\text{th}}$  subcarrier, and  $\epsilon(k) = \sqrt{0.5}$  for  $k = 0$  and 1 for  $k = 1, \dots, N-1$ .

### B. Optical Fast-OFDM system

The block diagram of the IM/DD Fast-OFDM combined with clipping and digital post-distortion is shown in Fig. 1. At the transmitter, after PAM mapping, the Fast-OFDM signal is generated using a length- $N$  IDCT and zero-padding (ZP) as guard interval. Then, amplitude clipping is employed to reduce the level of signal PAPR. After that, the Fast-OFDM signal is digital-to-analog converted (DAC), electrical amplified and transmitted over the IM/DD optical link. In this work, the optical link consists of a 1550-nm DFB laser source connected to a single-drive MZM, a 10-km single mode fiber (SMF), and a 50-GHz PIN photodiode. However, directly modulated DFB lasers (DMLs) or electro-absorption modulated lasers (EMLs) can also be used as optical transmitter. At the receiver side, the photo-detected signal is amplified and analog-to-digital converted. Then, the following DSP functions are employed: symbol synchronization (time alignment), digital post-distortion, Fast-OFDM demodulation based on a length- $2N$  FFT approach [16], channel estimation and zero-forcing equalization, and PAM de-mapping.

### C. Modeling approach

The measured data for the model extraction comes from the transmission of a 1.87-GHz Fast-OFDM signal over a 10-km length direct-detection optical link as described in [15], with the addition of a RF amplifier after the photodiode. The Fast-OFDM signal, used for model estimation only, is generated

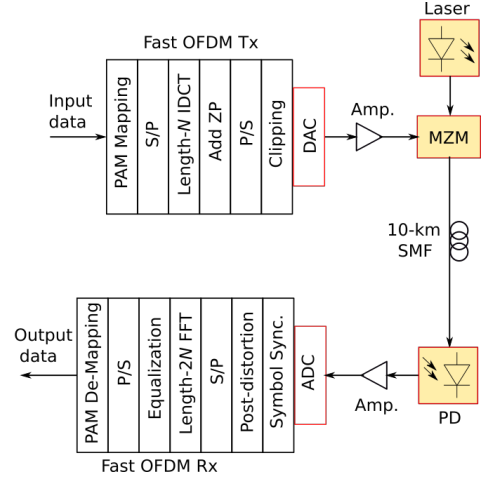


Fig. 1. Diagram of the IM/DD Fast-OFDM system.

with IDCT size of 512 and 192 data subcarriers modulated by four-level pulse amplitude modulation (4PAM) symbols. More details on the measurement setup can be found in [15]. In Matlab, the input-output Fast-OFDM signals are firstly time aligned and then the GMP model coefficients are estimated using the least-squares method, which estimates coefficients by minimizing the summed square of residuals. The output  $y_{GMP}$  of the GMP model is related to its input  $x$  by:

$$\begin{aligned} y_{GMP}(n) = & \sum_{k=1}^{K_a} \sum_{q=0}^{Q_a} a_{kq} x(n-q) |x(n-q)|^{k-1} \\ & + \sum_{k=2}^{K_b} \sum_{q=0}^{Q_b} \sum_{m=1}^{M_b} b_{kqm} x(n-q) |x(n-q-m)|^{k-1} \\ & + \sum_{k=2}^{K_c} \sum_{q=0}^{Q_c} \sum_{m=1}^{M_c} c_{kqm} x(n-q) |x(n-q+m)|^{k-1} \quad (2) \end{aligned}$$

Here, the first polynomial function is applied to time-aligned input signal samples, where  $K_a$  and  $Q_a$  are the nonlinearity order and the memory depth, respectively. The second polynomial function introduces cross-terms between the complex input signal and its lagging envelope terms up to the order of  $M_b$  and has a nonlinearity order  $K_b$  and memory depth of  $Q_b$ . The third polynomial introduces leading cross-terms up to the order of  $M_c$  and has a nonlinearity order and memory depth of  $K_c$  and  $Q_c$ , respectively. The parameters  $a_{kq}$ ,  $b_{kqm}$ , and  $c_{kqm}$  are the coefficients of the GMP model for the aligned terms, and the lagging and leading cross-terms, respectively. In this work, we use only odd-order nonlinear terms in the GMP model. Although the GMP is a nonlinear model, all of its coefficients can be easily estimated using any least-squares algorithm [13].

We also model the nonlinearity of the optical Fast-OFDM link using the MP model for comparison with the modeling accuracy obtained with the GMP. The MP model is given by

$$y_{MP}(n) = \sum_{k=1}^K \sum_{q=0}^Q a_{kq} x(n-q) |x(n-q)|^{k-1} \quad (3)$$

where  $x(n-q)$  is the input signal delayed by  $q$  sample periods,  $K$  is the nonlinearity order,  $Q$  is the memory length, and  $a_{kq}$  are the model coefficients. For a fair comparison with the GMP model, we use only odd-order nonlinear terms in the MP model.

#### D. Distortion compensation approach

In Fig. 2, a block diagram of the distortion compensation scheme for IM/DD Fast-OFDM links is shown. In this work, a simple amplitude clipping approach (without filtering) is used. For a Fast-OFDM signal  $x(n)$  and its clipped version  $x_c(n)$ , the clipping function is given by

$$x_c(n) = \begin{cases} x(n) & \text{if } |x(n)| \leq A_{th}, \\ A_{th}e^{j\theta} & \text{if } |x(n)| > A_{th}. \end{cases} \quad (4)$$

where  $\theta = \arg[x(n)]$ . The clipped signal is limited to the amplitude threshold  $A_{th}$  and the phase of  $x(n)$  is maintained in  $x_c(n)$ . By setting  $A_{th}$  to a lower value than the peak amplitude  $A_{max}$  of  $x(n)$ , the PAPR of the Fast-OFDM signal is reduced. Here, we define a clipping factor  $cf = A_{th}/A_{max}$ .

As shown in Fig. 2, the digital post-distorter is inserted after the IM/DD link (in baseband). It is trained for executing the inverse function of the optical link nonlinearity so that the complete system is linearized. Here, we do not use the GMP model as post-distorter as it has high complexity for real-time implementation. Instead, we use a simple memoryless polynomial function, with reduced number of coefficients obtained at the receiver side by using known 2PAM-Fast-OFDM training signals and a least squares (LS) fitting algorithm, provided by the “polyfit” function in MATLAB. High amplitude training signals, capable of sweeping all the link nonlinear characteristic, are used. In the diagram of Fig. 2, when the error  $e$  between the training signal  $x_{tr}$  and the output of the post-distorter training block  $\hat{x}_{tr}$  is minimized, the post-distorter coefficients are estimated by the training block and are then used to update the actual post-distorter. The post-distorted signal  $y_{pos}$  is then sent to the FFT-based demodulation and equalization, followed by the de-mapping block.

In Fig. 2, the output  $y_{pos}$  of the memoryless polynomial post-distorter is given by

$$y_{pos}(n) = \sum_{k=0}^K a_k y(n)^k \quad (5)$$

where  $y(n)$  is the baseband received signal,  $a_k$  are the model coefficients, and  $K$  is the polynomial order. In (5), we include both even- and odd-order nonlinear terms and set  $K$  to 3.

In this work, a block-based post-distortion training approach is adopted. With this approach, the training can be done in only one step and in a least-squares sense, avoiding the use of sample-by-sample algorithms. In addition, as previously proposed in [4], the received training signals are also post-distorted before being used for the FFT-based channel estimation and equalization. In this way, the memoryless polynomial based post-distortion approach has also a dynamic compensation effect on the system performance.

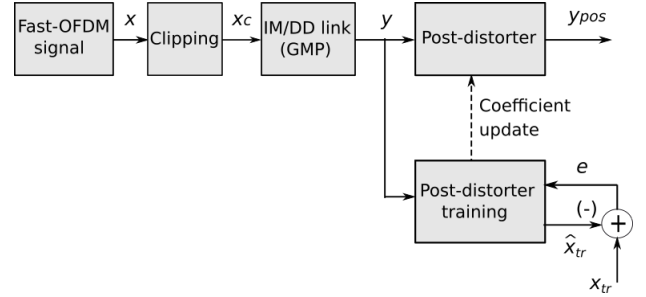


Fig. 2. The distortion compensation approach.

### III. MODELING AND SIMULATION RESULTS

#### A. Modeling accuracy results

We now compare the modeling accuracy of the odd-order GMP model against that of the odd-order MP model with approximately the same number of coefficients. The same Fast-OFDM measured data are used to estimate the GMP and MP model coefficients.

The modeling accuracy results are shown in Table I. By changing  $K_a$  and  $Q_a$  in (2) and  $K$  and  $Q$  in (3), we increase the number of coefficients for both models, proportionally. The other GMP model parameters are fixed at:  $K_b = 3$ ,  $Q_b = 1$ ,  $M_b = 1$ ,  $K_c = 5$ ,  $Q_c = 4$ , and  $M_c = 4$ . For memory length  $Q_a = 10$  or more and similar number of coefficients, the GMP model achieves better accuracy than the MP model. For  $Q_a = 20$ , the normalized mean square error (NMSE) of the GMP model is around 2 dB less than that of the MP model.

In Fig. 3, the measured and GMP modeled Fast-OFDM spectra are presented, while the MP modeled spectrum is shown in Fig. 4. It can be seen that a better agreement between the measured and modeled spectra is obtained using the GMP model.

TABLE I  
MODELING ACCURACY

| GMP model |    |             |           | MP model |    |             |           |
|-----------|----|-------------|-----------|----------|----|-------------|-----------|
| Ka        | Qa | No. Coeffs. | NMSE (dB) | K        | Q  | No. Coeffs. | NMSE (dB) |
| 3         | 5  | 45          | -22.44    | 3        | 22 | 46          | -23.84    |
| 3         | 10 | 55          | -25.30    | 3        | 27 | 56          | -23.86    |
| 3         | 15 | 65          | -25.90    | 3        | 32 | 66          | -23.97    |
| 3         | 20 | 75          | -25.95    | 3        | 37 | 76          | -23.87    |
| 5         | 5  | 51          | -22.46    | 5        | 16 | 51          | -23.94    |
| 5         | 10 | 66          | -25.33    | 5        | 21 | 66          | -23.97    |
| 5         | 15 | 81          | -25.94    | 5        | 26 | 81          | -23.99    |
| 5         | 20 | 96          | -25.98    | 5        | 31 | 96          | -24.01    |

#### B. Nonlinearity compensation results

In this section, the GMP model is applied to study the BER performance of clipping and digital post-distortion for MZM-based direct-detection optical Fast-OFDM systems, with a comparison against OFDM-based systems also included. The bandwidth of both the Fast-OFDM and OFDM signals is around 1.87 GHz. The ZP and cyclic prefix (CP) lengths of the Fast-OFDM and OFDM signals, respectively, are set to 1/32 of the corresponding IDCT and IFFT size. 2PAM-Fast-OFDM based training signals, with length of 10 symbols, are

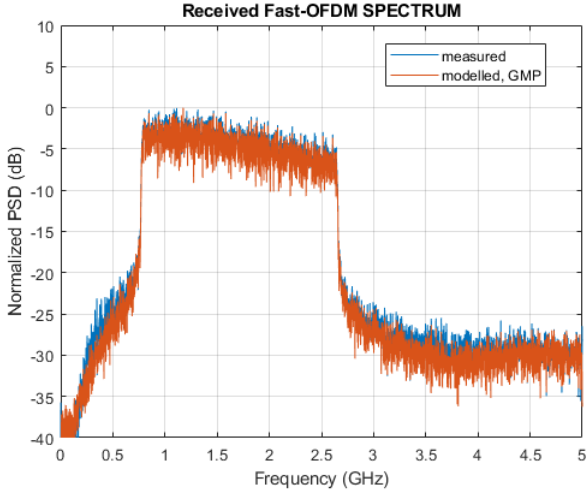


Fig. 3. Spectra of the measured and modeled Fast-OFDM signal. GMP model, 65 coefficients.

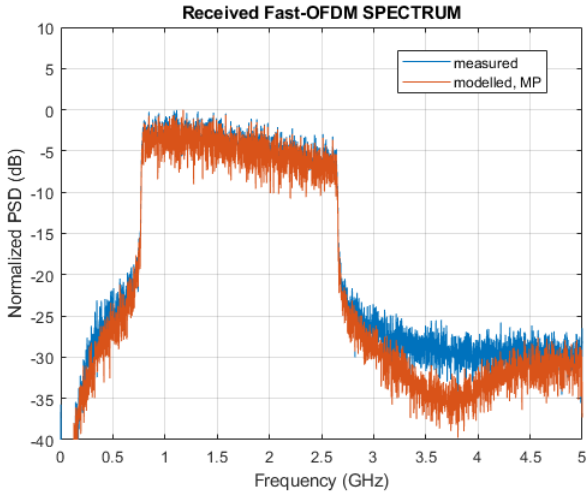


Fig. 4. Spectra of the measured and modeled Fast-OFDM signal. MP model, 66 coefficients.

used for both post-distortion training and frequency domain channel estimation. In the post-distorter model of (5),  $K$  is set to 3. The GMP model parameters in (2) are as follows:  $K_a = 3$ ,  $Q_a = 15$ ,  $K_b = 3$ ,  $Q_b = 1$ ,  $M_b = 1$ ,  $K_c = 5$ ,  $Q_c = 4$ , and  $M_c = 4$ . The total number of GMP coefficients is 65.

The BER results with/without distortion compensation for a 10-km length IM/DD 4PAM-Fast-OFDM link and considering the IDCT sizes  $N$  of 64, 128, and 256 are presented in Fig. 5. To maintain the same bit rate and signal bandwidth for all IDCT cases, the number of active (data) subcarriers is increased proportionally from 24 to 96. The average power level of the input Fast-OFDM signal is 13.5 dBm (before clipping) and a clipping factor (cf) of 0.8 is used. For each  $N$ -size IDCT, a post-distorter training signal with same  $N$  size is used. The BER performance of the 4PAM-Fast-OFDM with the proposed compensation approach is significantly better than that obtained using the conventional optical Fast-OFDM system. For example, at a BER level of  $10^{-3}$ , the required

SNR is reduced by around 3 dB and almost 5 dB due to the distortion compensation, for the IDCT sizes of 128 and 64, respectively. From Fig. 5, it can also be observed that the BER performance improves with increasing  $N$ . This is due to the reduction in the bandwidth of Fast-OFDM subcarriers, which improves the frequency domain equalization performance.

We now investigate the performance of the post-distortion approach for 8PAM-Fast-OFDM signals using the same 10-km length SMF-based GMP model and for  $N$  of 64, 128, and 256. The performance results are shown in Fig 6. In this case, no clipping is used as the 8PAM signal is very sensitive to the clipping-induced distortion. The input signal power level is 10.5 dBm. The results show that the post-distortion scheme can significantly improve the performance of 8PAM-Fast-OFDM signals at the higher  $E_b/N_0$  region in which the nonlinear effect of the IM/DD link is higher. For  $N = 64$ , BER below  $10^{-3}$  is achieved only if the post-distortion approach is employed. At the BER of  $10^{-3}$ ,  $E_b/N_0$  gains of more than 4 dB and almost 6 dB are achieved with post-distortion for  $N = 256$  and 128, respectively, in comparison to the conventional Fast-OFDM system with corresponding IDCT sizes.

In Fig. 7, the 8PAM received signal constellations after the 10-km IM/DD link, obtained using 10 training signals and for  $N = 256$ , are shown. It can clearly be observed the improvement in the signal constellation when the proposed digital compensation scheme is applied to the optical Fast-OFDM link.

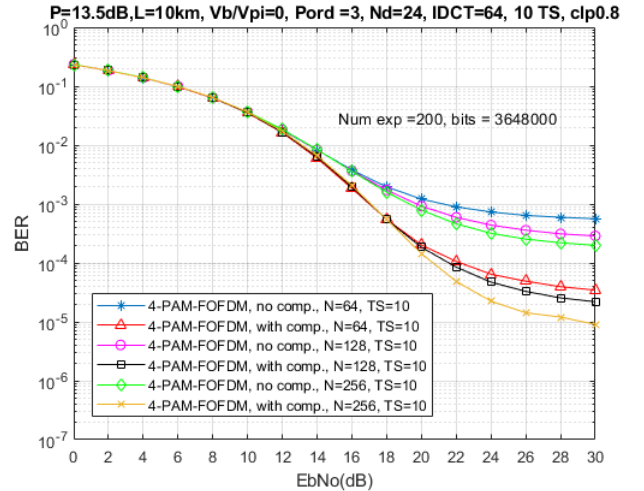


Fig. 5. BER performances with/without distortion compensation for the optical 4PAM-Fast-OFDM with different IDCT sizes ( $N$ ).

In Fig. 8, the BER results with/without distortion compensation for optical 4PAM-Fast-OFDM and 16QAM-OFDM systems are compared. The performances of the Fast-OFDM and OFDM systems are evaluated using GMP-based optical Fast-OFDM and OFDM link models, respectively. Both link models have the same structure and number of coefficients and were extracted from the same 10-km SMF link. The results are obtained for an IDCT of 64, an input signal with power level of 13.5 dBm, and a clipping factor of 0.8. The bit rates of the 4PAM-Fast-OFDM and the 16QAM-OFDM links are equal. For the non compensated link cases, the performances of the

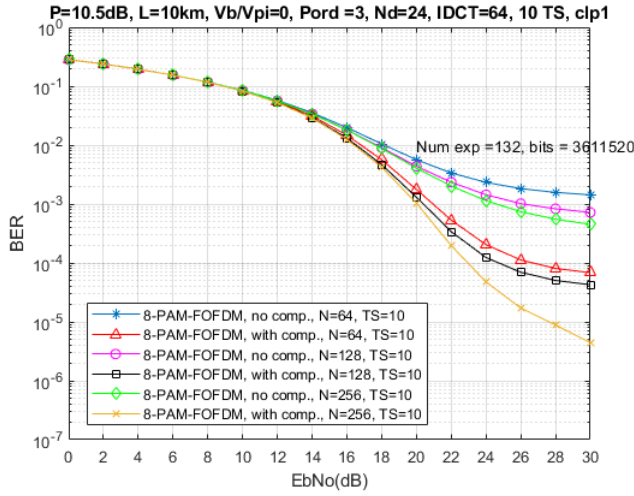


Fig. 6. BER performances with/without distortion compensation for the optical 8PAM-Fast-OFDM with different IDCT sizes ( $N$ ).

Fast-OFDM and OFDM systems are almost the same. When the distortion compensation is applied, the 4PAM-Fast-OFDM outperforms the 16QAM-OFDM at the higher  $E_b/N_0$  region.

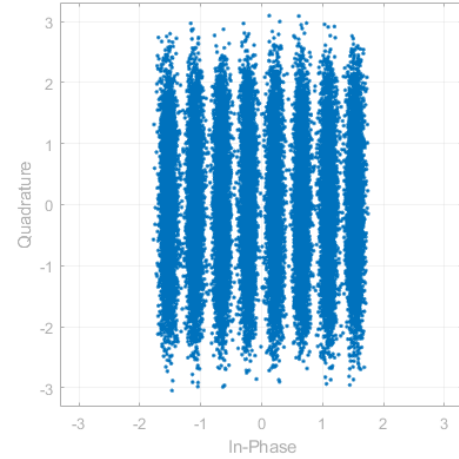
#### IV. CONCLUSION

In this work, we study the accuracy of the GMP for the modeling of nonlinear and memory effects of optical Fast-OFDM systems. To the best of our knowledge, this is the first time that the GMP model is used as a dynamic nonlinear representation of such a system. In addition, we combine a simple clipping approach with digital post-distortion for nonlinearity compensation of optical Fast-OFDM systems. We also propose using 2PAM-based training signals for both digital post-distortion and frequency domain channel estimation of 8PAM-Fast-OFDM links, with excellent performance results reported.

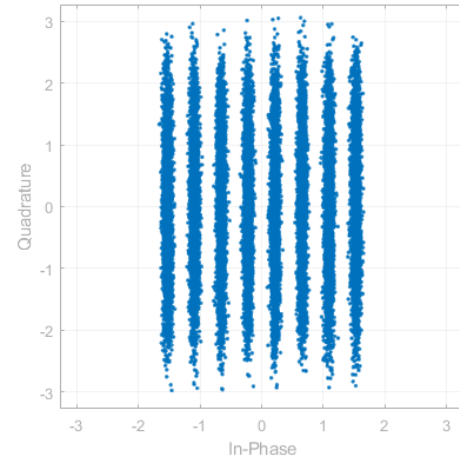
The GMP-based modeled spectrum shows an excellent agreement with the measured Fast-OFDM spectrum. In comparison to the MP model, for similar number of coefficients, better modeling accuracy is obtained using the GMP model, for a memory length of 10 or more.

The BER results show that the combination of clipping and digital post-distortion can significantly improve the system performance of a 10-km SMF IM/DD 4PAM-Fast-OFDM link, with SNR gain of almost 5 dB achieved (at a BER of  $10^{-3}$ ) in comparison to conventional optical Fast-OFDM. For the case of 8PAM-Fast-OFDM, this study indicates that better performance improvement can be obtained by using only digital post-distortion (without clipping). At the BER of  $10^{-3}$ , a SNR gain of almost 6 dB is achieved when digital post-distortion is applied to a 10-km SMF IM/DD 8PAM-Fast-OFDM link, for an IDCT size of 128.

The BER performances of the IM/DD Fast-OFDM and conventional OFDM systems with and without clipping/post-distortion have also been compared, for the same bit rate. When the distortion compensation approach is used, the 4PAM-Fast-OFDM system outperforms the 16QAM-OFDM at the higher SNR region. We emphasize that, even when the



(a)



(b)

Fig. 7. 8PAM received constellations for  $N = 256$ : (a) without distortion compensation, (b) with distortion compensation.

optical Fast-OFDM and OFDM achieve similar error rates, the Fast-OFDM system offers simpler implementation due to the real arithmetic operations.

#### REFERENCES

- [1] J. Ma, J. He, M. Chen, Y. Liu, Z. Zhou, and K. Wu, "Enhanced performance of PS-256QAM-OFDM for optical access network," *Optics Communications*, vol. 467, p. 125566, 2020. [Online]. Available: <http://www.sciencedirect.com/science/article/pii/S0030401820301760>
- [2] D. Zou, Y. Chen, F. Li, Z. Li, Y. Sun, L. Ding, J. Li, X. Yi, L. Li, and Z. Li, "Comparison of bit-loading DMT and pre-equalized DFT-spread DMT for 2-km optical interconnect system," *Journal of Lightwave Technology*, vol. 37, no. 10, pp. 2194–2200, 2019.
- [3] M. Rodrigues and I. Darwazeh, "Fast OFDM: A proposal for doubling the data rate of ofdm schemes," in *Proc. IEEE/IEE Int. Conf. Telecommun.*, 06 2002.
- [4] L. C. Vieira, S. Hussein, I. Darwazeh, C.-P. Liu, and J. Mitchell, "A combined digital linearization and channel estimation approach for IM/DD fast-OFDM systems," *Optical Fiber Technology*, vol. 67, p. 102725, 2021.
- [5] Z. Zhou, J. He, J. Ma, and M. Chen, "Experimental demonstration of an SFO-robustness scheme with fast OFDM for IMDD passive optical network systems," *Journal of Lightwave Technology*, pp. 1–1, 2020.
- [6] Z. Zhou, J. He, J. Ma, Y. Xiao, and Y. Cheng, "Adaptive modulation scheme for DML-based IM/DD FOFDM systems using overlap

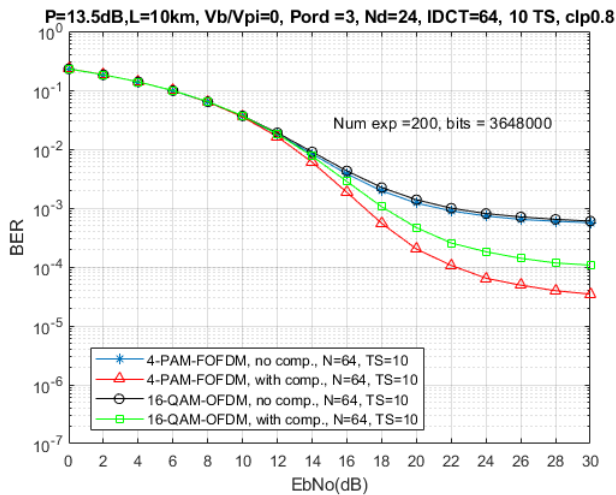


Fig. 8. BER performances with/without distortion compensation for 4PAM-Fast-OFDM and 16QAM-OFDM IM/DD systems.

frequency-domain equalization,” *Optical Fiber Technology*, vol. 48, pp. 213–217, 2019.

- [7] E. Giacomidis, S. K. Ibrahim, J. Zhao, J. M. Tang, A. D. Ellis, and I. Tomkos, “Experimental and theoretical investigations of intensity-modulation and direct-detection optical Fast-OFDM over MMF-links,” *IEEE Photonics Technology Letters*, vol. 24, no. 1, pp. 52–54, 2012.
- [8] T. Jiang and Y. Wu, “An overview: Peak-to-average power ratio reduction techniques for OFDM signals,” *IEEE Transactions on Broadcasting*, vol. 54, no. 2, pp. 257–268, 2008.
- [9] T. Lee and H. Ochiai, “On limitation of clipping and filtering in IEEE 802.11g based wireless LAN system,” in *WAMICON 2011 Conference Proceedings*, 2011, pp. 1–5.
- [10] H. Qian, S. J. Yao, S. Z. Cai, and T. Zhou, “Adaptive postdistortion for nonlinear LEDs in visible light communications,” *IEEE Photonics Journal*, vol. 6, no. 4, pp. 1–8, 2014.
- [11] C. Mateo, J. Clemente, P. Garcia-Ducar, P. L. Carro, J. de Mingo, and I. Salinas, “Digital predistortion of a full-duplex radio-over-fiber mobile fronthaul link with feedback loop,” in *2017 13th International Wireless Communications and Mobile Computing Conference (IWCMC)*, 2017, pp. 1425–1430.
- [12] L. C. Vieira and N. J. Gomes, “Experimental demonstration of digital predistortion for orthogonal frequency-division multiplexing-radio over fibre links near laser resonance,” *IET Optoelectronics*, vol. 9, no. 6, pp. 310–316, 2015.
- [13] D. Morgan, Z. Ma, J. Kim, M. Zierdt, and J. Pastalan, “A generalized memory polynomial model for digital predistortion of RF power amplifiers,” *IEEE Transactions on Signal Processing*, vol. 54, no. 10, pp. 3852–3860, 2006.
- [14] L. Ding, G. Zhou, D. Morgan, Z. Ma, J. Kenney, J. Kim, and C. Giardina, “A robust digital baseband predistorter constructed using memory polynomials,” *IEEE Transactions on Communications*, vol. 52, no. 1, pp. 159–165, 2004.
- [15] L. C. Vieira, I. Darwazeh, S. Hussein, C.-P. Liu, and J. Mitchell, “Experimental demonstration of direct-detection optical Fast-OFDM using memory polynomials,” in *2021 IEEE Latin-American Conference on Communications (LATINCOM)*, 2021, pp. 1–5.
- [16] X. Ouyang and J. Zhao, “Single-tap equalization for fast OFDM signals under generic linear channels,” *IEEE Communications Letters*, vol. 18, no. 8, pp. 1319–1322, 2014.